# COORDINATION CHART FOR COLLISION-FREE MOTION OF TWO ROBOT ARMS

*You-shik Shin, and Zeungnam Bien

Dept. of Electrical Engineering, KAIST
P. O. Box 150, Chongyangni, Seoul, KOREA

## Abstract

When a task requires two robot arms to move in a cooperative manner sharing a common workspace, potential collision exists between the two robot arms. In this paper, a novel approach for collision-free trajectory planning along paths of two SCARA-type robot arms is presented. Specifically, in order to describe potential collision between the links of two moving robot arms along the designated paths, an explict form of "Virtual Obstacle" is adopted, according to which links of one robot arm are made to grow while the other robot arm is forced to shrink as a point on the path. Then, a notion of "Coordination Chart" is introduced to visualize the collision-free relationship of two trajectories.

## 1. Introduction

When a task requires two robot arms to move in a cooperative manner sharing a common workspace, potential collision exists between the two robot arms. Thus, some kinds of motion coordination between the two robot arms should be incorporated for an efficient multi-robot system.

Different from the case of stationary obstacle with a single robot arm(1,2,3), regarding collision-free motion planning for multi-robot system, relatively little work has been reported so far. Freund et al.(4) formulated problem of collision avoidance in multi-robot system as a findpath problem and suggested an algorithm with some simulation results. Kant et al.(5) solved the trajectory planning problem in time varying environments for a point robot. In their method, problem of planning collision-free trajectory is decomposed into two subproblems of path finding with stationary obstacles and velocity planning along the path to avoid collision with moving obstacles. In order to plan collision-free velocity profile along the chosen path, they first transformed potential collision into path-time space using the path information of a point robot and trajectory of moving obstacles, and algorithms are then presented to solve the velocity planning problem with different optimality criteria. Lee et al.(6) proposed an approach to collision-free motion planning for two moving robots using a sphere model for the wrist of the robot, straight line trajectory planning, and notions of a collision map and time scheduling. In time scheduling of a trajectory, using speed reduction and/or time delay of the robot motion, an algorithm is presented to achieve collision-free trajectory.

In this paper, a novel approach for collision-free trajectory planning along paths of two SCARA-type robot arms is presented. For this, in Section 2, a basic theory of obtaining virtual obstacle of given arbitrary shaped stationary obstacle is discussed first. Then explicit form of virtual obstacle is presented in Section 3. To visualize all the collision-free relation of two trajectories, in Section 4, a notion of coordination chart is introduced, and the conclusions are drawn in Section 5.

## 2. Basic theory with stationary obstacle

Consider a robot arm with two links driven by two revolute joints in series. As usual, the links of the robot arm are modelled as solid lines as shown in Fig. 1. $l_1$ and $l_2$ denote the lengths of the first and the second link, respectively, and $l_1>l_2$ is assumed. By convention, $\theta_1$ and $\theta_2$, angles of rotation for joint 1 and joint 2, respectively, are positive if measured in the clockwise direction.

Let $D_1$ and $D_2$ be the sets of allowable joint angles of joint 1 and joint 2 of robot arm, respectively, and it is assumed that

$$D_1=\{\theta_1 | -\pi<\theta_1\leq\pi\} \quad (1)$$

$$D_2=\{\theta_2 | -\pi\leq\theta_2\leq 0\}. \quad (2)$$

Since the robot arm has only two degrees of freedom, the position and orientation can be specified by either a single two-dimensional vector, called its configuration, $\theta=(\theta_1,\theta_2)^T$, or position vector $X=(x,y)^T$, where T denotes the transpose operation and x and y are coordinates of end-effector along the x- and y-axis with respect to the origin o.

Let the robot arm be denoted as R. We use the notation $R_X$ to be the set of all points (x,y) in the Cartesian x-y space such that each (x,y) belongs to the first line link or the second link of the robot arm in a particular configuration $\theta=(\theta_1,\theta_2)^T$ corresponding to a position vector X.

Now, given an obstacle $A_i$ described as a set in the Cartesian space, we will denote $V(A_i)$ to mean the set in the Cartesian space of all position vectors of R which collides with the obstacle $A_i$.

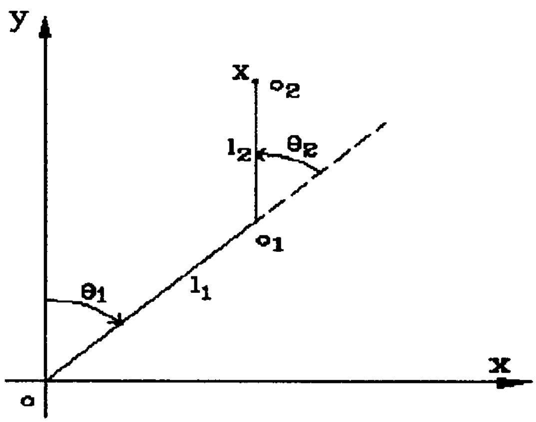


Fig. 1 Robot arm R

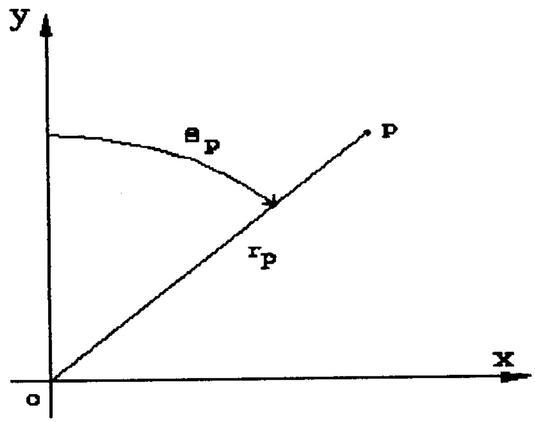


Fig. 2 Point obstacle p

i.e.,

$$V(A_i)=\{X|R_X \cap A_i \neq \emptyset\}. \quad (3)$$

$V(A_i)$ is simply called the "virtual" obstacle for the corresponding obstacle $A_i$. Then we can obtain the following result.

**Theorem 1:**
For robot arm R in a particular position X,

$$R_X \cap A_i = \emptyset \iff X \cap V(A_i) = \emptyset.$$

Implication of Theorem 1 is that when the robot arm is in a particular position X, the necessary and sufficient condition for the robot arm $R_X$ being free from collision with obstacle $A_i$ is that point X is free from collision with virtual obstacle $V(A_i)$.

**Theorem 2:**
Let A be the union of finite number n of obstacles $A_i$'s, i.e., $A=\bigcup_{i=1}^{n} A_i$. Then,

$$V(A)=\bigcup_{i=1}^{n} V(A_i).$$

**Theorem 3:**
Let $B_i$ be the boundary of obstacle $A_i$. Then, $V(B_i)=V(A_i)$.

Based on the above Theorem 2 and Theorem 3, a simple procedure of obtaining the virtual obstacles V(A) can be summarized as follows:

**Step 1):** Set index: i=1.
**Step 2):** For $A_i$, find $V(B_i)$.
**Step 3):** Update the index: i=i+1.
**Step 4):** If $i \leq n$ then go to Step 2, otherwise proceed to Step 5.
**Step 5):** Now, $V(A)=\bigcup_{i=1}^{n} V(B_i)$.

As can be noticed, Step 2 of finding $V(B_i)$ needs further refinements. To this end, a method of finding the virtual obstacle for a point obstacle is detailed in the next section.

**3. Virtual obstacle for a point obstacle**

A point obstacle p in the Cartesian space can be described completely in the polar coordinate system as $(r_p, \theta_p)$, where $r_p$ is the distance of the point p from the origin and $\theta_p$ is the angle between the y-axis and the straight line segment op as shown in Fig. 2. By convention, $\theta_p$ is positive if measured in the clockwise direction.

For the point obstacle p, various forms of virtual obstacle V(p) can be generated depending on its location. It is found that there are five distinct cases according to the location of point obstacle p.

**Case 1:** $r_p=0$

When the obstacle p is at the origin of the Cartesian space, whole workspace of R becomes virtual obstacle from the definition of (3).

**Case 2:** $0<r_p<l_1-l_2$

The first link of R is in collision with p only when $\theta_1=\theta_p$, regardless of $\theta_2$ as shown in Fig. 3.a. Thus, the virtual obstacle in this case is half circle, i.e.,

$$V(p)=\{X=(x,y)^T|(x-l_1\sin\theta_p)^2+(y-l_1\cos\theta_p)^2 = l_2^2 \text{ and } x-y\tan\theta_p \leq 0\}. \quad (4)$$

Fig. 3.b shows the virtual obstacle for a point obstacle p for the case of $r_p$=5.29 cm and $\theta_p$=45° with $l_1$=37 cm, and $l_2$=23 cm.

**Case 3:** $l_1-l_2 \leq r_p \leq l_1$

In this case, there are possibilities that both the first and/or the second link may collide with p. When the first link collides with p, the virtual obstacle can be described by the same equation as in (4).

$$V(p)_1=\{X=(x,y)^T|(x-l_1\sin\theta_p)^2+(y-l_1\cos\theta_p)^2 = l_2^2 \text{ and } x-y\tan\theta_p \leq 0\}. \quad (5)$$

When only the second link collides with p as illustrated in Fig 4.a, the virtual obstacle is

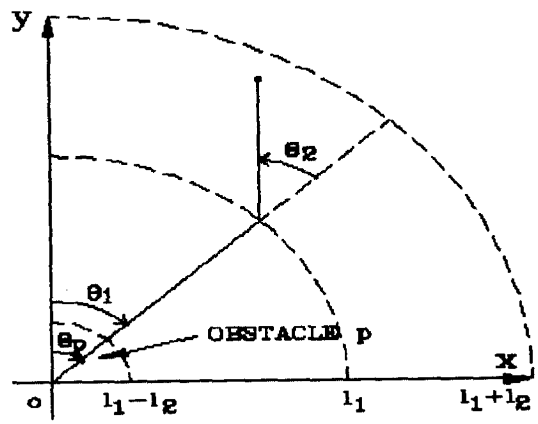


Fig. 3.a $0<r_p<l_1-l_2$ case

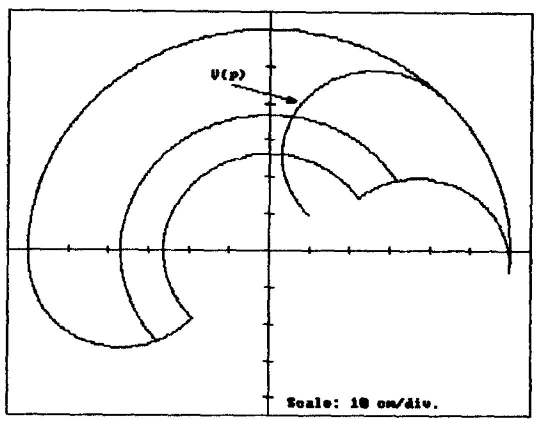


Fig. 3.b V(p) when p=(5.29cm,45°)

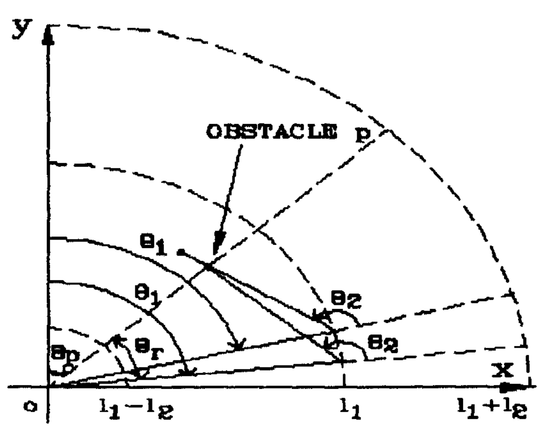


Fig. 4.a $l_1-l_2\le r_p\le l_1$ case

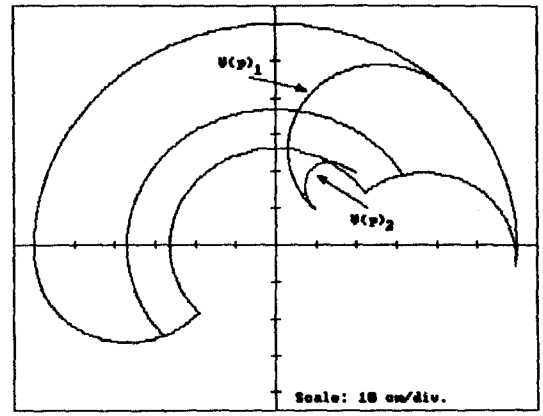


Fig. 4.b V(p) when p=(28cm,45°)

given by

$$V(p)_2=\{X=(x,y)^T \mid \sqrt{(x-x_p)^2+(y-y_p)^2}+\sqrt{(x_p-x_1)^2+(y_p-y_1)^2}=l_2 \text{ and } x-y\tan\theta_p\le 0\} \quad (6)$$

where $x_1=l_1\sin\theta_1$, $y_1=l_1\cos\theta_1$ with $\theta_p\le\theta_1\le\theta_p+\theta_r$ and $\theta_r=\cos^{-1}\dfrac{r_p^2+l_1^2-l_2^2}{2r_pl_1}$. $\theta_r$ is the angle between op and the first link when the end point of the second link of R is in collision with p. It should be noted that $\theta_r$ is positive.

Summarizing, the virtual obstacle in this case is

$$V(p)=V(p)_1\cup V(p)_2. \quad (7)$$

In Fig. 4.b, is shown the virtual obstacle for a point obstacle of $r_p$=28 cm and $\theta_p$=45° with the link parameters being the same as in Case 2.

**Case 4:** $l_1<r_p\le l_1+l_2$

In this case, only the second link can potentially collide with p as shown in Fig. 5.a. The virtual obstacle, in this case, is the same as in (6) as depicted in Fig. 5.b for a point obstacle of $r_p$=45 cm and $\theta_p$=45° with the link parameters as in Case 2.

**Case 5:** $l_1+l_2<r_p$

In this case, a point obstacle can not limit the movement of robot arm R. Thus virtual obstacle is empty, i.e.,

$$V(p)=\emptyset. \quad (8)$$

Now, since the boundary of a given obstacle $A_i$(not necessarily a point obstacle) can be thought as the union of infinite number of point obstacles of boundary points, the virtual obstacle $V(A_i)$ for $A_i$ can be obtained by examining all the boundary points of $A_i$ according to the above five cases.

Fig. 6.a shows an example. In this case, the obstacle is a straight line which is parallel to x-axis and located at y=29 cm. The corresponding virtual obstacle in Fig. 6.b is illustrated for the case of $l_1$=37 cm and $l_2$=23 cm.

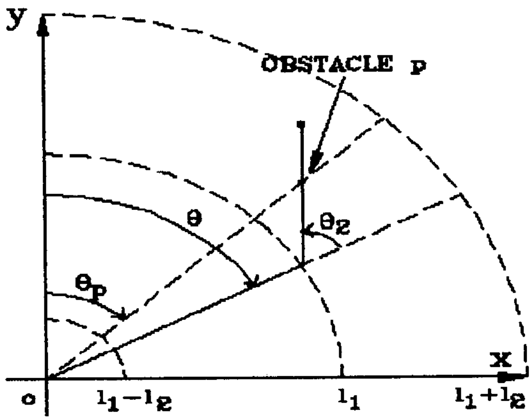


Fig. 5.a $l_1 < r_p \le l_1 + l_2$ case

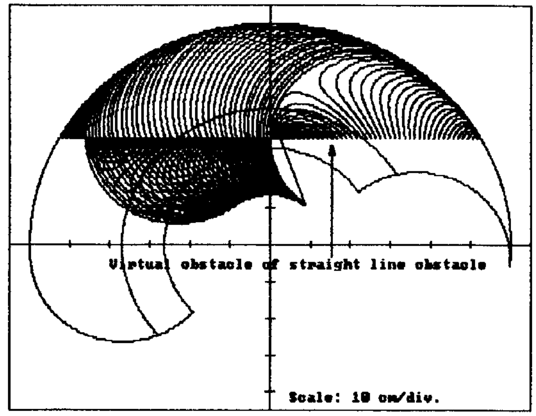


Fig. 6.b Virtual obstacle of straight line

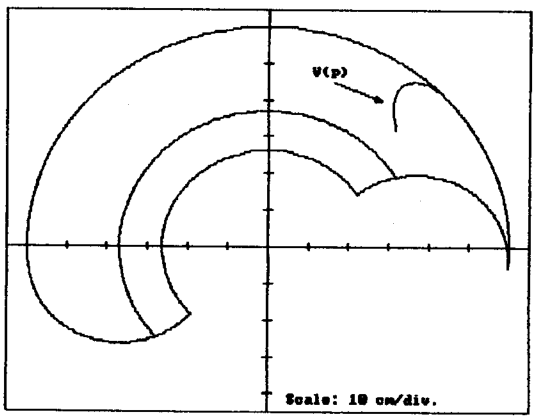


Fig. 5.b V(p) when p=(45cm, 45°)

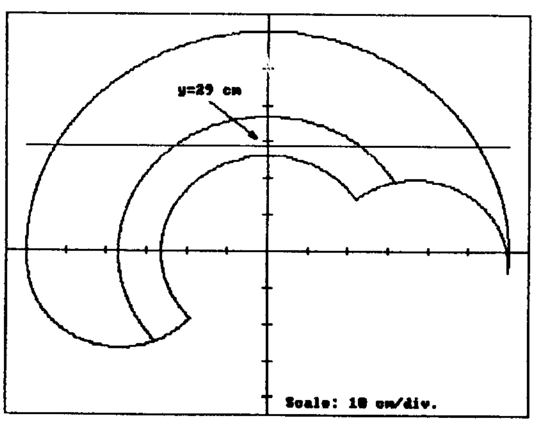


Fig. 6.a Straight line obstacle

## 4. Coordination chart for collision avoidance

Consider two SCARA-type robot arms working in a cooperative manner sharing a common workspace as shown in Fig. 7. In Fig. 7, robot 1 and robot 2 are to move from their respective initial points denoted as i's to the final points f's along the designated paths, which are not necessarily straight lines. It is obvious that collision between the links of the robot 1 and the robot 2 can occur depending on relative movement of both robot arms. For example, consider the following trivial cases. If the robot 2 starts when the robot 1 completes its movement, for the robot 2 there is no way of going to the final point f along the designated path without collision. On the other hand, if the robot 2 completes first, and then the robot 1 starts, there is no collision at all regardless of trajectory of the robot 1. Considering case that the two robot arms move simultaneously, situation becomes rather complex. It is remarkable that in this case, each robot arm acts as moving and shape-varying obstacle with respect to the other robot arm. Therefore, in this section, a notion of "coordination chart" is introduced to tell(, or visualize) all the collision-free relationship of two trajectories for the two moving robot arms.

### (1) Coordination chart

Let $s_1$ and $s_2$ be normalized traveled distances along the designated paths of the robot 1 and the robot 2, respectively, then $s_1, s_2 \in [0,1]$. Now consider two-dimensional $s_1 \times s_2$ space, the Cartesian product space of $s_1$ and $s_2$. The basic idea is that from the path information of the two robot arms, using the concept of the virtual obstacle of Section 2 and Section 3, we can represent all the potential collision between the two moving robot arms on the $s_1 \times s_2$ space. The $s_1 \times s_2$ space with potential collision region on it is simply called coordination chart.

To apply the concept of virtual obstacle, regarding the robot 2 in Fig. 7 as the robot R considered in Section 2 and Section 3, let us shrink the robot 2 as a point on the end-effector

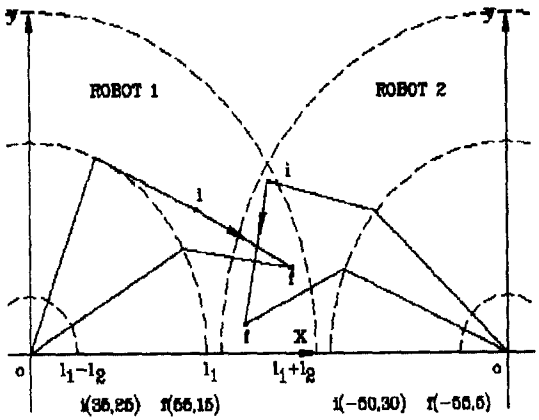


Fig. 7 Two robot arms

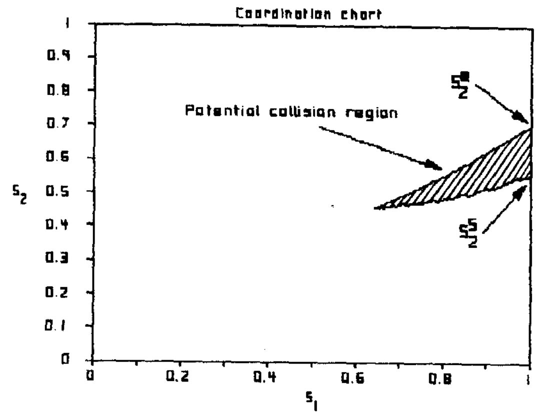


Fig. 9 Coordination chart

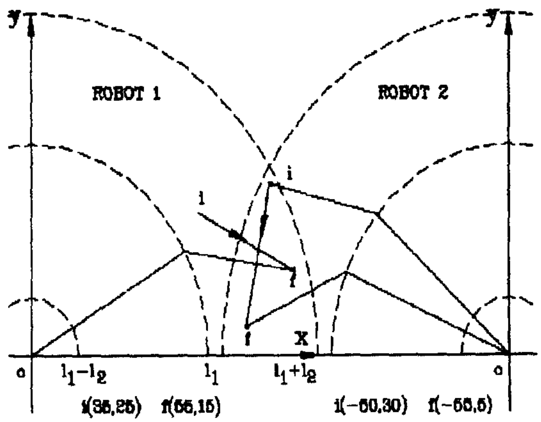


Fig. 8.a $s_1$=1 case

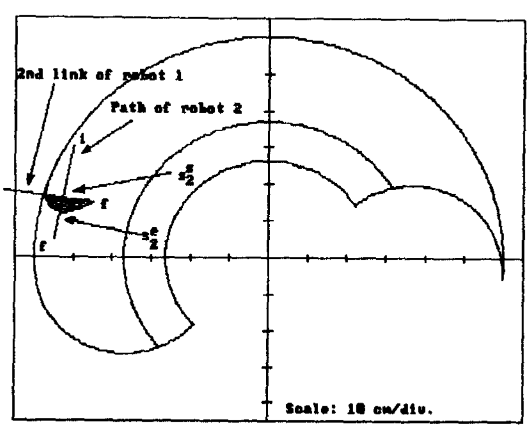


Fig. 8.b Collision segment when $s_1$=1

of the robot 2 which is also a point on the given path of the robot 2 while obtaining the virtual obstacle of the portion of the robot 1 in the common workspace. Case when the robot 1 is at its final point, i.e., $s_1$=1, is depicted in Fig. 8.a. Applying (4)-(8) to every point on the links of the robot 1 which is also in the common workspace, the virtual obstacle can be obtained as shown in Fig. 8.b. In this figure, collision start and end points on the path of the robot 2 is denoted as $s_2^s$ and $s_2^e$, respectively and this collision segment of $s_2 \in [s_2^s, s_2^e]$ when $s_1$=1 can be mapped into $s_1 \times s_2$ space as shown in Fig. 9. Now, repeating the same procedure described above along every point on the path of the robot 1, i.e., varying $s_1$ from 0 to 1, we can obtain the final coordination chart as in Fig. 9.

**(2) Collision-free relation of two trajectories**

Using the notion of coordination chart, we actually converted two robot arms as a point on the $s_1 \times s_2$ space. Depending on the path requirement of the two robot arms, we can actually obtain various types of coordination chart. If, however, points (0,0) and (1,1) on the coordination chart are not connected as in Fig. 10.a, then there is no way of accomplishing their tasks for the both robot arms along the designated paths. Fig 10.b shows the case that the robot 2 begins starting when the robot 1 completes its movement and Fig 10.c shows the converse situation. Denoting collision-free relation of the robot 1 with respect to the robot 2 and the vice versa as f and g respectively, i.e., $s_1=f(s_2)$ and $s_2=g(s_1)$, it can be remarked that both the collision-free relation f and g must be monotone increasing each other, otherwise either one of the two robot arms moves backward along the given path as in Fig 10.d and Fig 10.e. In Fig 10.d and Fig 10.e, the robot 1 and the robot 2 moves backward temporarily and this situation is not desirable in the practical sense.

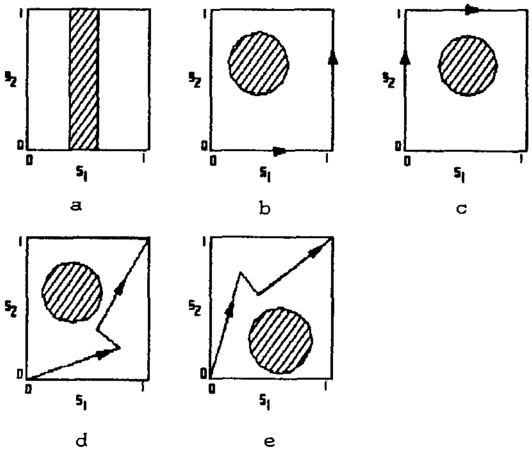


Fig. 10 Collision-free relation

## 5. Conclusions

A novel idea of coordination chart was presented for collision-free trajectory planning problem of two robot arms along the given paths, which are not necessarily straight lines. In order to effectively describe potential collision between the links of two robot arms, an explicit form of virtual obstacle was adopted for the SCARA-type robot arm. Via the coordination chart, all the collision-free trajectory relationship between two moving robot arms could be visualized. Finally, it can be remarked that idea of virtual obstacle can be equally applicable to other types of contemporary robot arm such as a combination of prismatic and revolute-type one or only prismatic-type robot arm.

## Reference


1. T. L. Perez, "Automatic planning of manipulator transfer movements," IEEE trans. Syst., Man, Cybern., vol. SMC-11, no. 6, Oct. 1981.

2. R. A. Brooks, "Planning collision-free motions for pick-and-place operations," Int. J. Robotics Research, vol. 2, no.4, Winter 1983.

3. J. Y. S. Luh, and C. E. Campbell, "Minimum distance collision-free path planning for industrial robots with a prismatic joint," IEEE trans. Automat. Contr., vol. AC-29, no. 8, Aug. 1984.

4. E. Freund, and H. Hoyer, "Collision avoidance in multi-robot systems," in Proc. 2nd Int. Sympos. Robotics Research, 1984, pp 135-146.

5. K. Kant, and S. W. Zucker, "Toward efficient trajectory planning: The path-velocity decomposition," Int. J. Robotics Research, vol. 5, no. 3, Fall 1986.

6. B. H. Lee, and C. S. G. Lee, "Collision-free motion palnning of two robots," IEEE trans. Syst., Man, Cybern., vol. SMC-17, no. 1, Jan./Feb. 1987.